Supporting Information

Interfacial Engineering of $CoMoO_4$@MoS_2/CoS_2 Heterostructure for Enhancing Electrochemical Nitrate Reduction to Ammonia

Xiaoyang Yang[a], Wei Jiang[a], Xin Cui[a], Guangping Lei[b], Haoyu Qiu[a], Zeyi Liu[a], Jiafeng Wan[a] and Yifu Liu[a], Fangwei Ma[a,*]

[a] Key Laboratory of Chemical Engineering Processes & Technology for High-efficiency Conversion (College of Heilongjiang Province), School of Chemistry and Material Science, Heilongjiang University, Harbin 150080, China.

[b] School of Energy and Power Engineering, North University of China, Taiyuan 030051, China

*E-mail address: fangwei_ma@hotmail.com

Ion concentration detection method (Product analysis.)

Use the colorimetric method to determine the concentrations of nitrite and ammonia[1–3]. Use a UV visible spectrophotometer (UV-VIS spectroscopy) to detect the absorbance of the electrolyte diluted to the appropriate concentration, and compare the calibration curve to calculate the ion concentration. The specific detection method is as follows:

Determination of NO_2^-

The concentration of NO_2^- in the electrolyte was evaluated using the Griess test. First, Griess reagent was prepared by adding 1 mL of H_3PO_4, 0.02 g of N-(1-naphthalene)-ethylenediamine dihydrochloride, and 0.4 g of sulfanilamide to 10 mL of deionized water. 0.1 mL of electrolyte was taken and diluted to 5 mL with deionized water (50 times), and 0.1 mL of color developer was added. After standing

for 20 min, the absorbance curve was measured in the wavelength range of 400 ~ 700 nm and the absorbance value of 540 nm was selected. The standard curve was measured with a series of $NaNO_2$ solutions of different concentrations to calculate the NO_2^- yield and FE.

Calculation of NO_2^- yield and Faradaic efficiency

$$NO_2^- \text{ yield } (\mu mol\ h^{-1}\ mg^{-1}) = \frac{c_{NO_2^-} \times V}{M \times t \times m}$$

$$\text{Faradaic efficiency} = \frac{n \times F \times c_{NO_2^-} \times V}{M \times Q \times 1000} \times 100\%$$

where n is the number of electrons transferred (n=2), F =96485 C mol^{-1} is the Faraday constant, $c_{NO_2^-}$ (μg mL^{-1}) is the measured NO_2^- concentration, V (mL) is the volume of NO_2^- cathodic reaction electrolyte, M=46 is the relative molecular mass of products, Q (C) is the total quantity of applied electricity.

Determination of NH_3：

The concentration of ammonia produced was determined by the indophenol blue spectrometer method. Then, 2 mL of diluted electrolyte, 2 mL of 1 M Na OH solution (5% salicylic acid and 5% sodium citrate), 1 mL of 0.05 M NaClO, and 0.2 mL of 1% sodium nitroferricyanide (III) dihydrate ($C_5FeN_6Na_2O \cdot 2H_2O$) solution were mixed. After standing for 2 h away from light, the absorbance was recorded on a UV-visible (UV-VIS spectroscopy) spectrophotometer at an absorption spectrum at a wavelength of 655 nm. The standard curve was determined with a series of NH_4Cl solution of different concentrations to calculate the NH_3 yield and FE.

Calculation of NH_3 yield and Faradaic efficiency:

$$NH_3 \text{ yield } (\mu mol\ h^{-1}\ mg^{-1}) = \frac{c_{NH_3} \times V}{M \times t \times m}$$

$$\text{Faradaic efficiency} = \frac{n \times F \times c_{NH_3} \times V}{M \times Q \times 1000} \times 100\%$$

where n is the number of electrons transferred (n=8), F=96485 C mol^{-1} is the Faraday constant, c_{NH_3} (μg mL^{-1}) is the measured NH_3 concentration, V (mL) is the

volume of NH_3 cathodic reaction electrolyte, M=17 is the relative molecular mass of products, m is the amount of catalyst supported, Q (C) is the total quantity of applied electricity and t (h) is the reduction time.

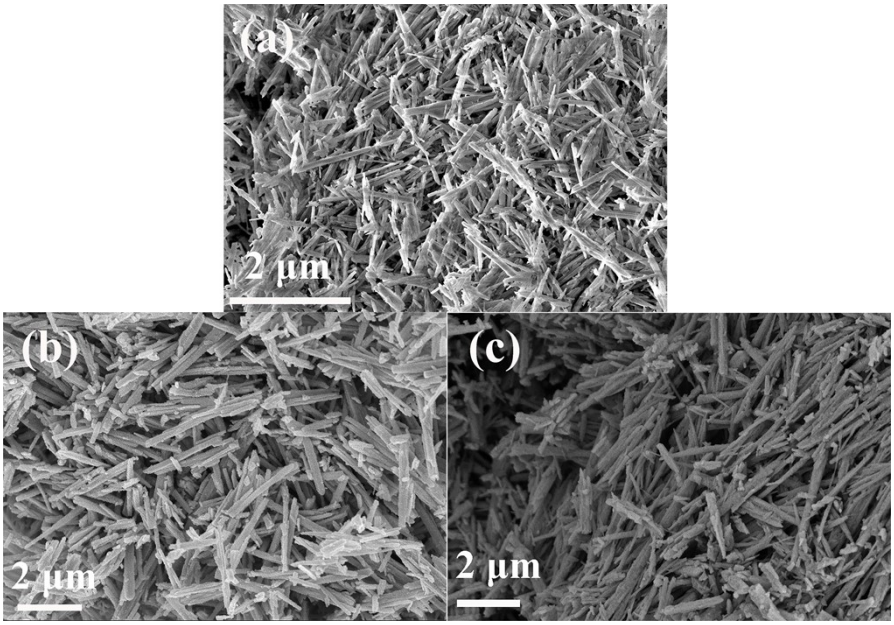

Fig. S1 SEM images of (a) $CoMoO_4$, (b) $CoMoO_4$@MoS_2/CoS_2-5 and (c) MoS_2/CoS_2.

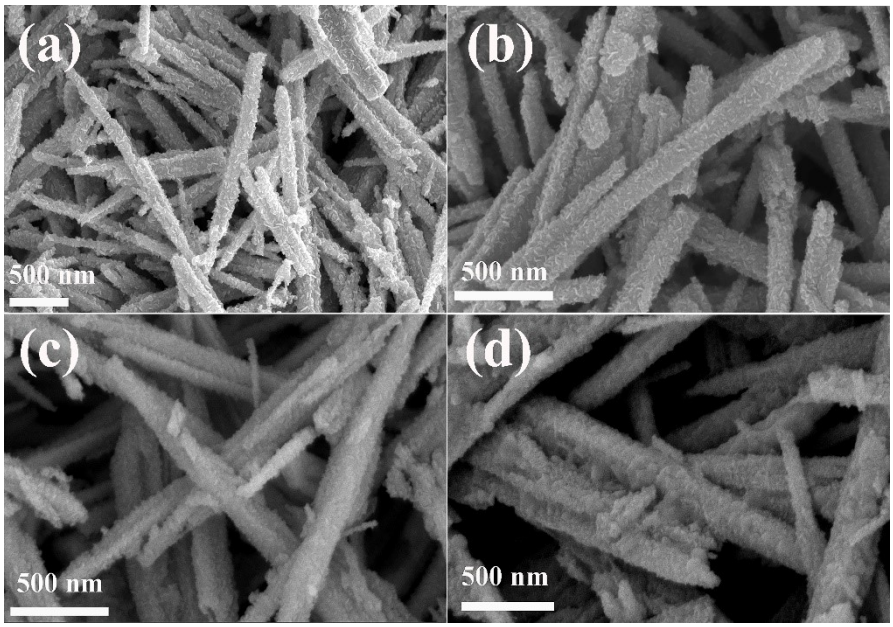

Fig. S2 SEM images of (a) $CoMoO_4$@MoS_2/CoS_2-3, (b) $CoMoO_4$@MoS_2/CoS_2-5, (c) $CoMoO_4$@MoS_2/CoS_2-7, and (d) MoS_2/CoS_2.

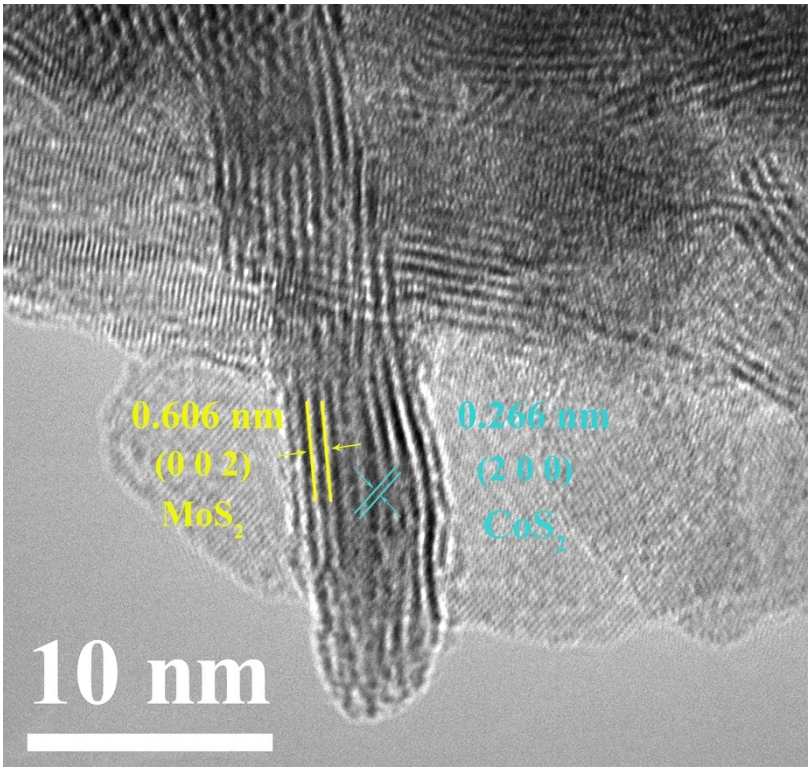

Fig. S3 The high-resolution TEM image on the edge of $CoMoO_4$@MoS_2/CoS_2-5.

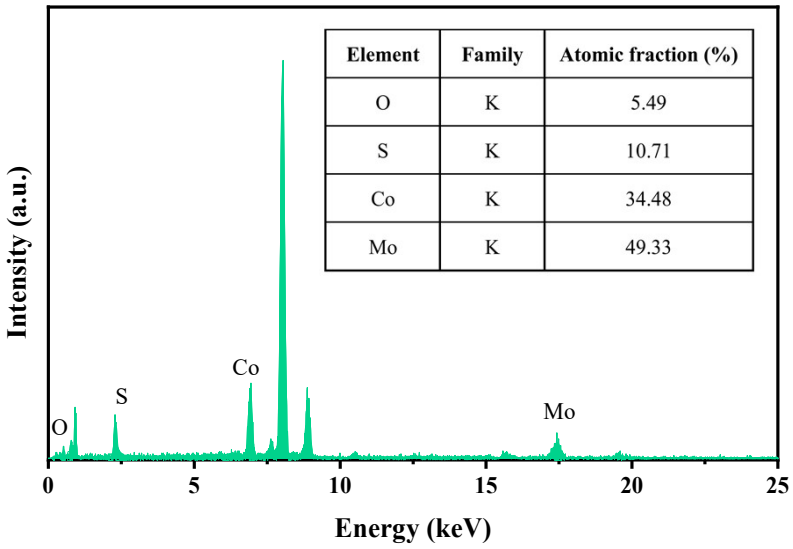

Fig. S4 EDX spectra for $CoMoO_4$@MoS_2/CoS_2-5.

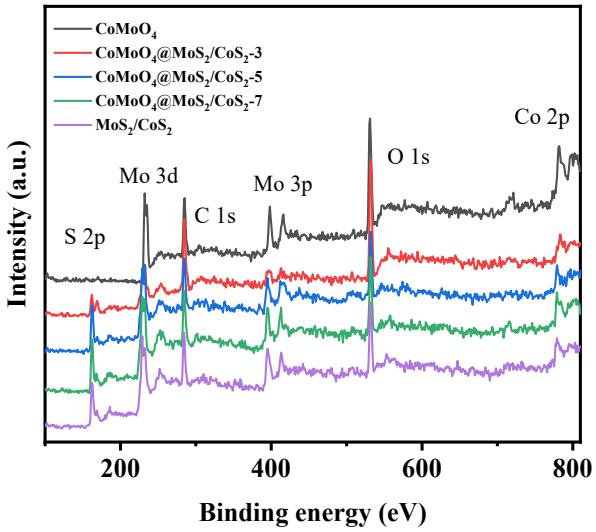

Fig. S5 XPS survey spectrums of $CoMoO_4$, $CoMoO_4$@MoS_2/CoS_2-3, $CoMoO_4$@MoS_2/CoS_2-5, $CoMoO_4$@MoS_2/CoS_2-7, and MoS_2/CoS_2.

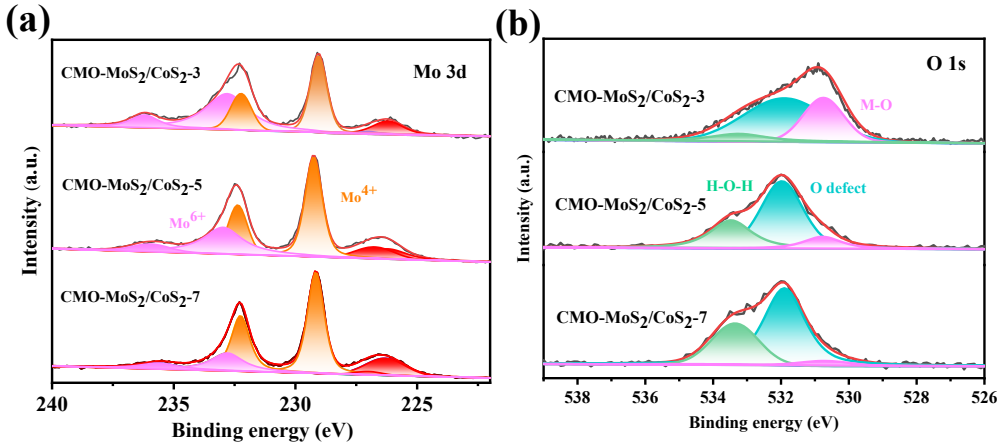

Fig. S6 High-resolution XPS spectra of (a) Mo 3d, (b) O 1s for $CoMoO_4$@MoS_2/CoS_2-3, $CoMoO_4$@MoS_2/CoS_2-5, and $CoMoO_4$@MoS_2/CoS_2-7.

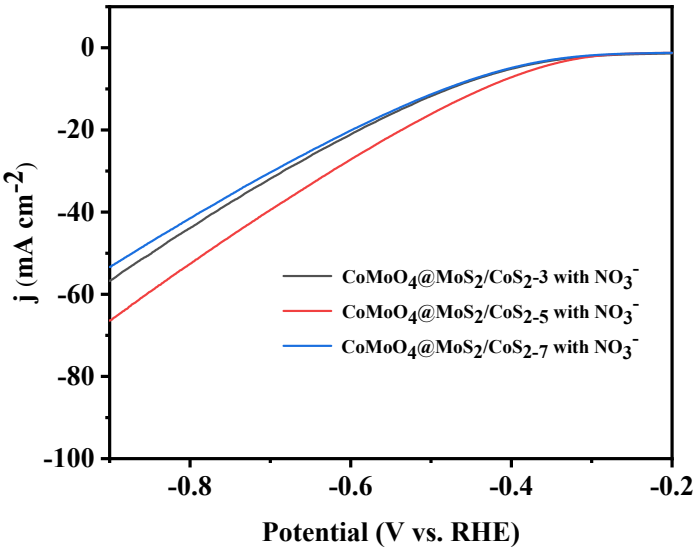

Fig. S7 LSV curves of (a) $CoMoO_4$@MoS_2/CoS_2-3, (b) $CoMoO_4$@MoS_2/CoS_2-5 and (c) $CoMoO_4$@MoS_2/CoS_2-7 in 0.5 M Na_2SO_4 with 0.1 M $NaNO_3$.

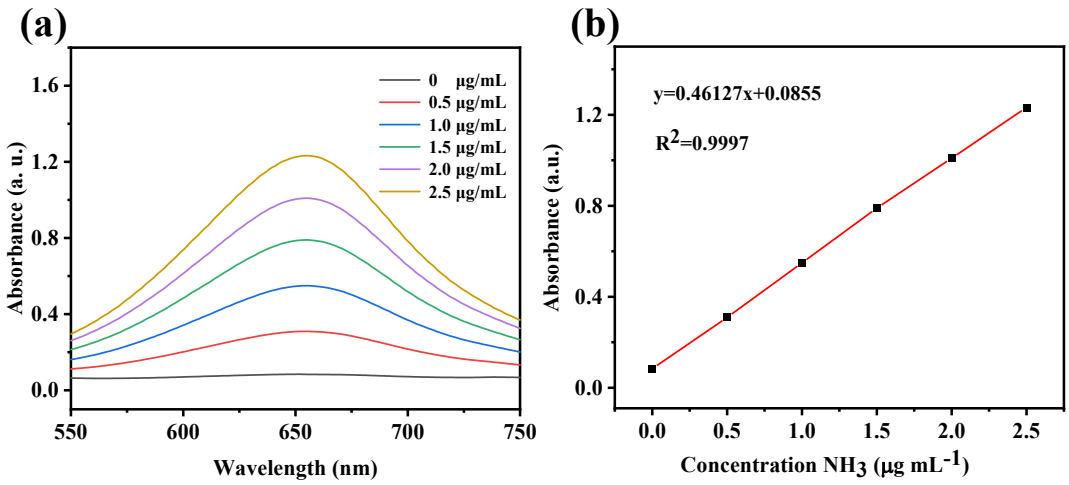

Fig. S8 (a) UV-Vis absorption spectra and (b) calibration curve for determining NH_3.

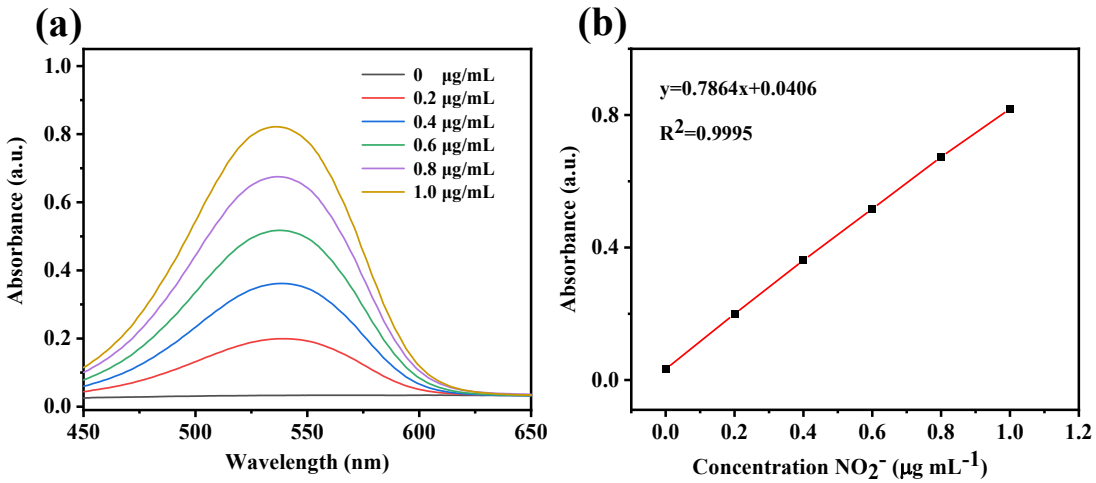

Fig. S9 (a) UV-Vis absorption spectra and (b) calibration curve for determining NO_2^-.

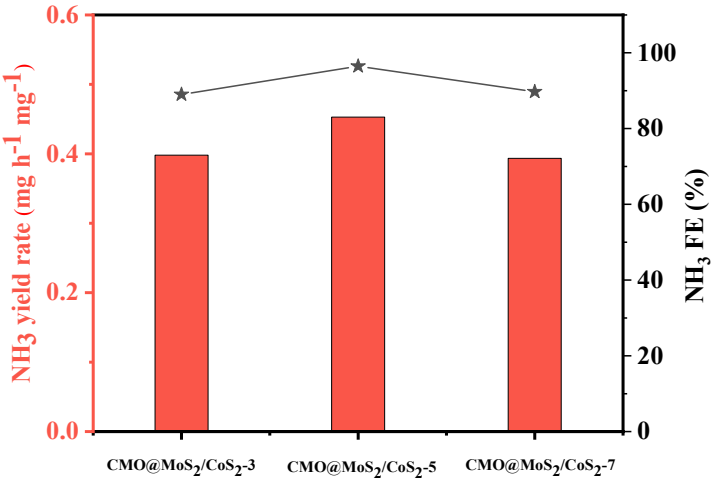

Fig. S10 NH_3 yield rate and FE of $CoMoO_4$@MoS_2/CoS_2-3, $CoMoO_4$@MoS_2/CoS_2-5, and $CoMoO_4$@MoS_2/CoS_2-7 at -0.8 V.

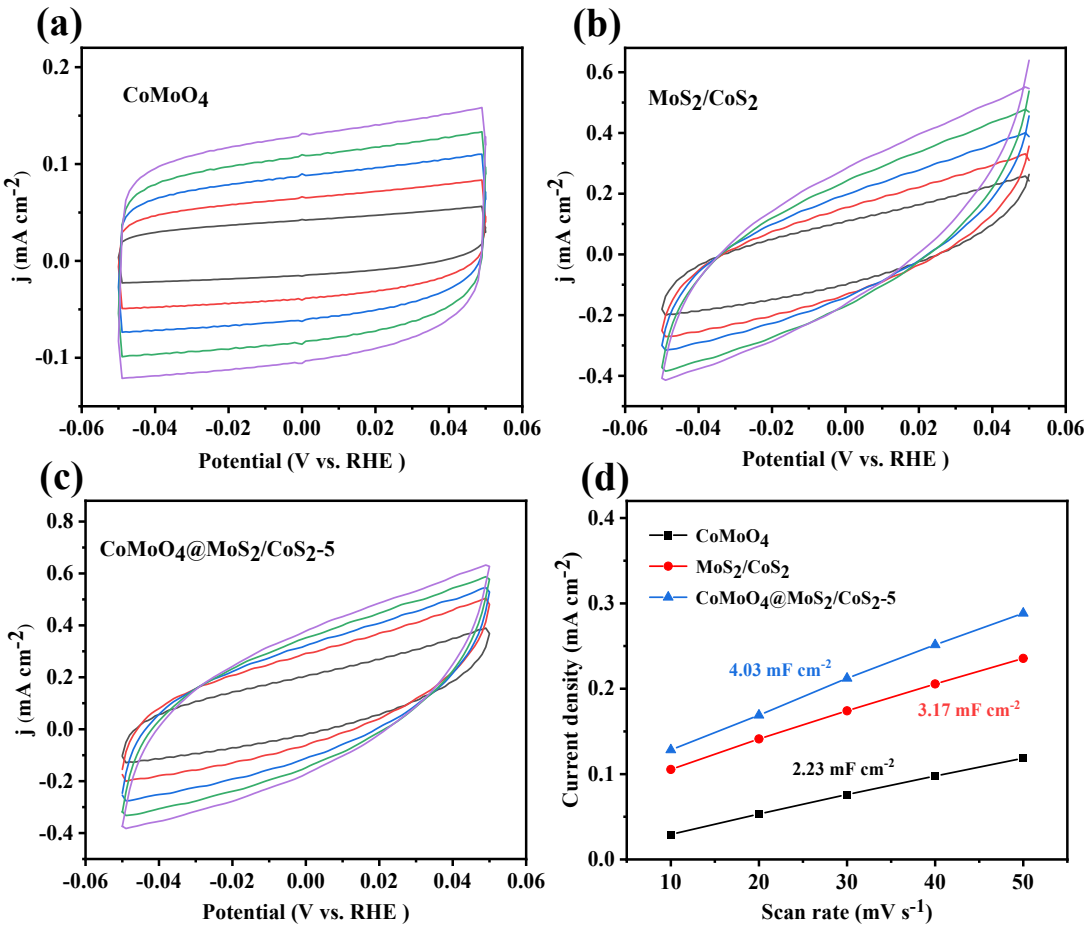

Fig. S11 CV results for the (a) $CoMoO_4$, (b) MoS_2/CoS_2, and (c) $CoMoO_4@MoS_2/CoS_2$-5 at scan rates of 10, 20, 30, 40, and 50 mV s^{-1}, and (d) the electrochemical double-layer capacitance (C_{dl}).

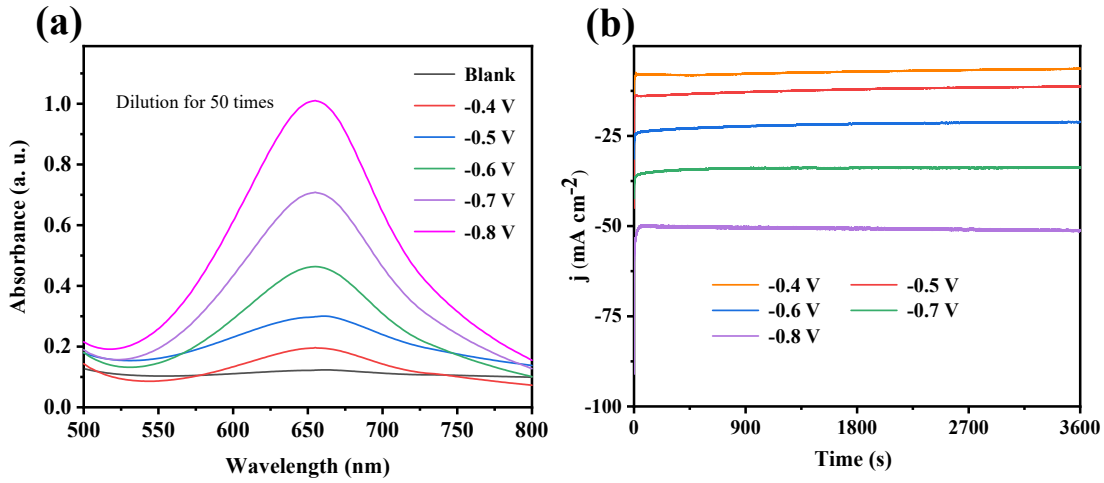

Fig. S12(a) UV−vis absorption spectra and (b) Time-dependent current density curves of $CoMoO_4@MoS_2/CoS_2$-5 for NO_3RR at different given potentials.

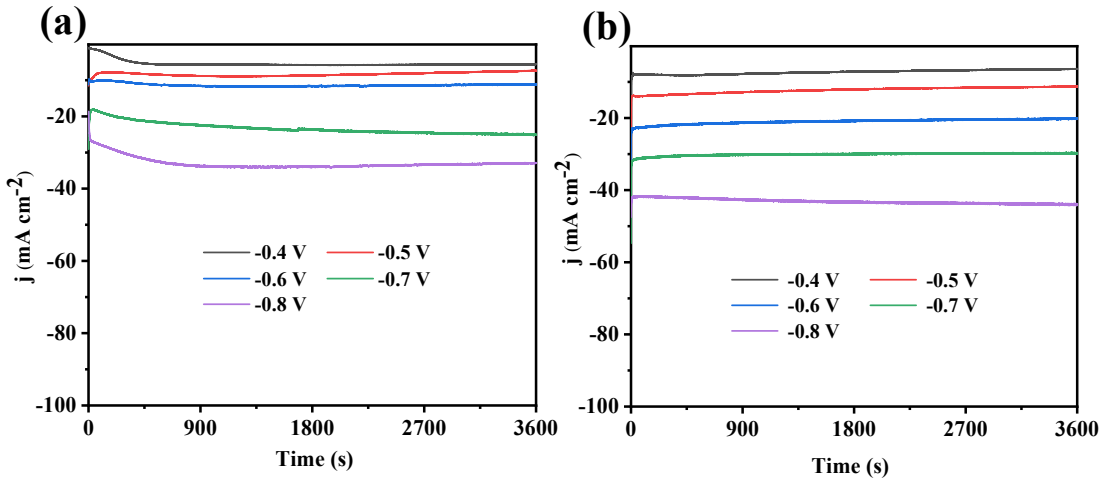

Fig. S13 Time-dependent current density curves of (a) $CoMoO_4$ and (b) MoS_2/CoS_2 for NO_3RR at different given potentials.

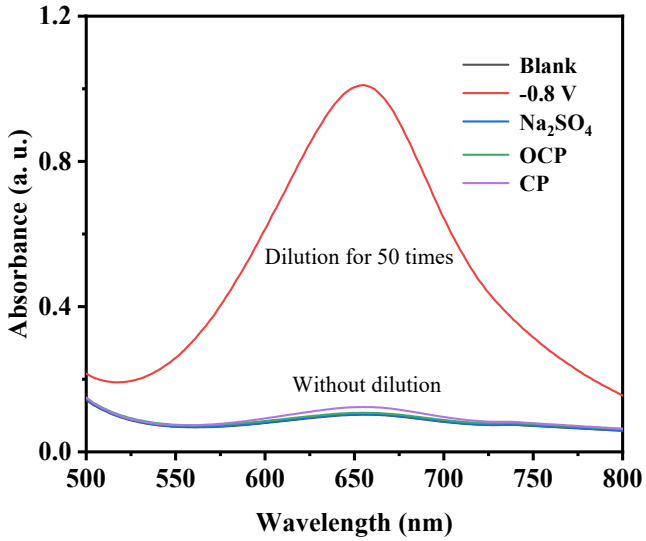

Fig. S14 UV-Vis absorption spectra of NH_3 after 1 h of NO_3RR at different conditions.

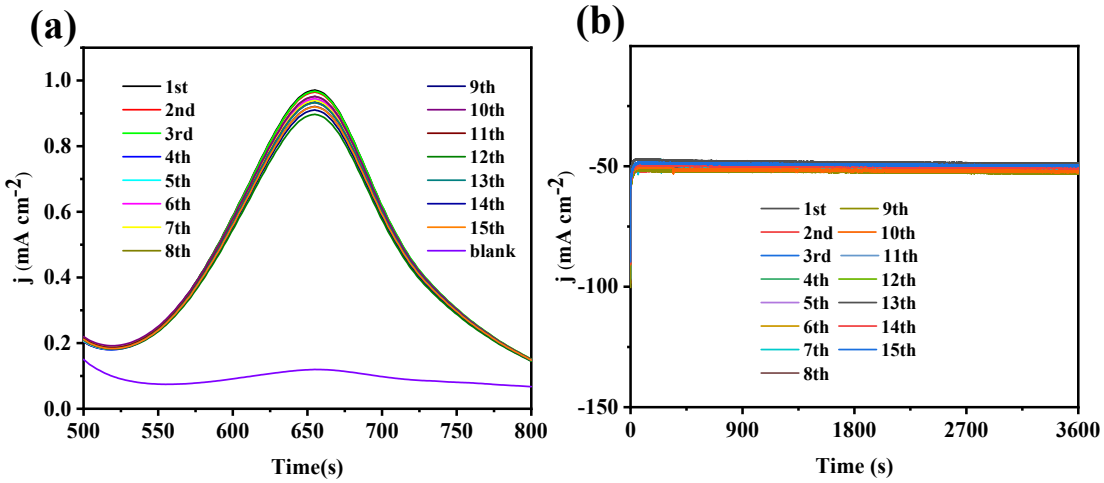

Fig. S15 (a) UV-Vis absorption spectra and (b) Time-dependent current density curves of $CoMoO_4$@MoS_2/CoS_2-5 for recycling test.

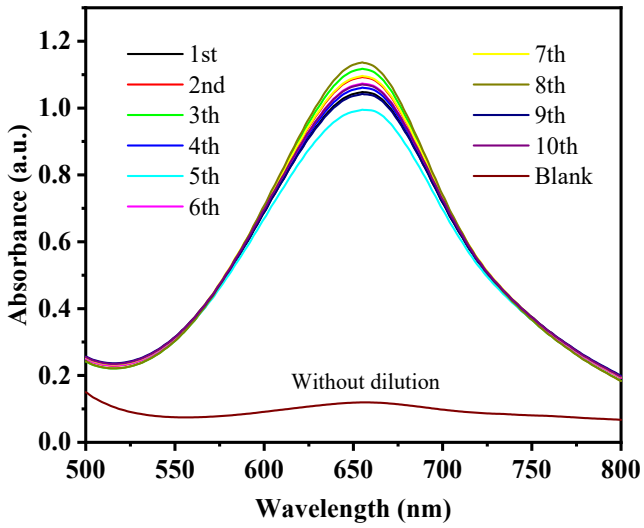

Fig. S16 UV-Vis absorption spectra of $CoMoO_4$@MoS_2/CoS_2-5 for long-time test.

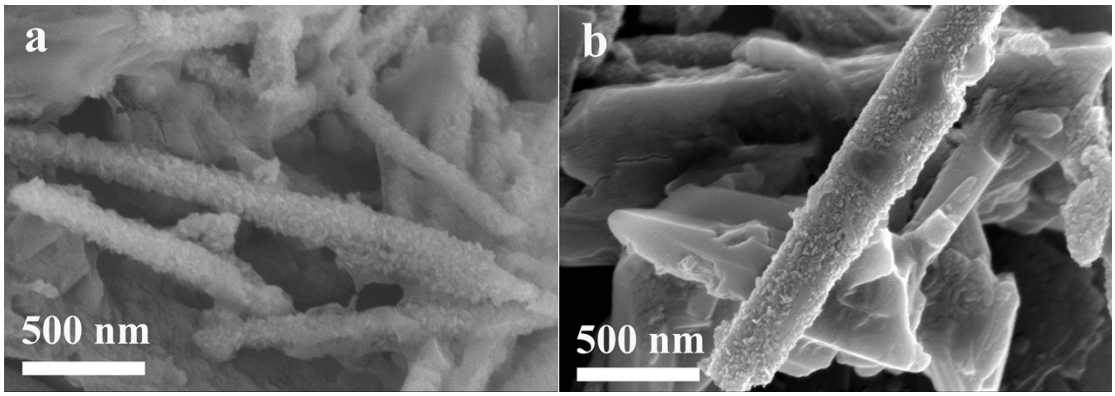

Fig. S17 SEM of $CoMoO_4$@MoS_2/CoS_2-5 before and after long-time test.

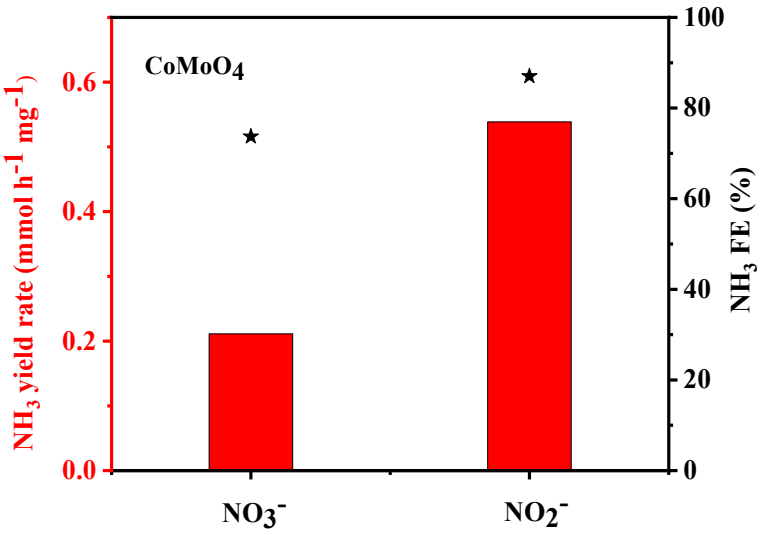

Fig. S18 The NH_3 yield rate and FE for $CoMoO_4$ in 0.1 M NO_3^- and 0.05 M NO_2^- electrolyte at -0.8 V.

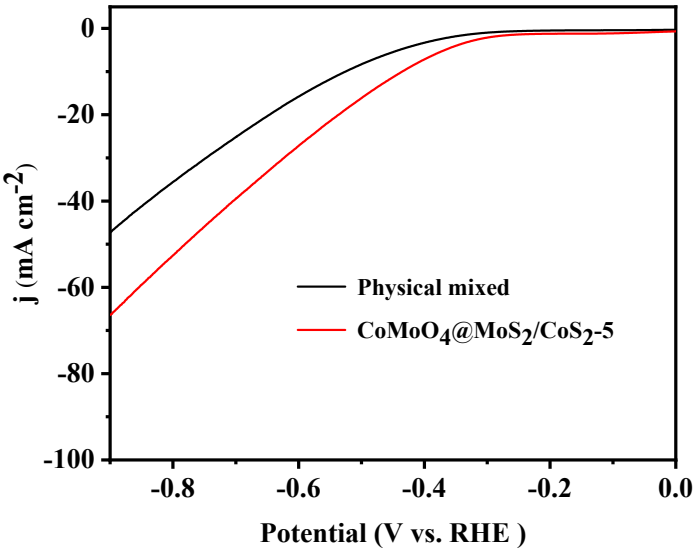

Fig. S19 LSV curves of physical mixed sample and $CoMoO_4$@MoS_2/CoS_2-5 in 0.5 M Na_2SO_4 and 0.1 M $NaNO_3$ solution.

Table S1. Summary of some recent electrocatalysts reported for NH_3 synthesis by NO_3^-RR.

Catalyst	Electrolyte	NH_3 yield rate	FE (%)	Potential (V vs RHE)	Ref.
$CoMoO_4$@MoS_2 /CoS_2	0.5 M Na_2SO_4 (0.1 M NO_3^-)	0.45 mmol $h^{-1}mg^{-1}$	96.11	-0.8	This work
Bi_2S_3/MoS_2	0.1 M Na_2SO_4 (0.1 M NO_3^-)	0.15 mmol h^{-1} cm^{-2}	88.4	-0.8	4
Co–NCNT	0.1 M NaOH (0.1 M NO_3^-)	6 mg $h^{-1}cm^{-2}$	92.08	-0.6	5
MoO_2-C NBF	1 M KOH (0.1 M NO_3^-)	0.11 mmol h^{-1} cm^{-2}	99.05	-0.3	6
MoS_2/CoS_2	1 M KOH (600 ppm NO_3^-)	0.44 mmol h^{-1} cm^{-2}	97.07	-0.25	7
$CoMoO_4$	0.1 M Na_2SO_4 (200 ppm NO_3^-)	0.16 mmol h^{-1} cm^{-2}	93.33	-0.7	8
Co_3O_4@CoBi	0.1 M PBS (0.1 M NO_3^-)	4.13 mg h^{-1} cm^{-2}	97	-0.7	9
Ce-MoS_{2-x}/CC	0.5 M Na_2SO_4 (0.1 M NO_3^-)	7.3 mg h^{-1} cm^{-2}	96.6	-0.7	10
$CuCo_2O_4$/CFs	0.1 M KOH (0.1 M NO_3^-)	0.39 mmol h^{-1} cm^{-2}	81.9	-0.3	11

Table S2. Calculation method for theoretical performance of the physical mixed sample

	Yield rate (Y, mmol h^{-1} mg^{-1})		FE (%)		
	NH_3	NO_2^-	NH_3	NO_2^-	H_2
$CoMoO_4$	0.21688	0.01328	70.11	1.62	28.27
MoS_2/CoS_2	0.34554	0.12006	85.87	7.46	6.67
Calculation	0.303	0.084	80.62	5.51	13.87

$$Y_{Calculation} = \frac{1}{3}Y_{CoMoO_4} + \frac{2}{3}Y_{MoS_2/CoS_2}$$

$$FE_{Calculation} = \frac{1}{3}FE_{CoMoO_4} + \frac{2}{3}FE_{MoS_2/CoS_2}$$

Supplementary references

(1) Cui, X.; Tang, C.; Zhang, Q. A Review of Electrocatalytic Reduction of Dinitrogen to Ammonia under Ambient Conditions. *Advanced Energy Materials* **2018**, *8* (22), 1800369. https://doi.org/10.1002/aenm.201800369.

(2) Mao, R.; Zhu, H.; Wang, K.; Zhao, X. Selective Conversion of Nitrate to Nitrogen Gas by Enhanced Electrochemical Process Assisted by Reductive Fe(II)-Fe(III) Hydroxides at Cathode Surface. *Applied Catalysis B: Environmental* **2021**, *298*, 120552. https://doi.org/10.1016/j.apcatb.2021.120552.

(3) Yang, K.; Han, S.-H.; Cheng, C.; Guo, C.; Li, T.; Yu, Y. Unveiling the Reaction Mechanism of Nitrate Reduction to Ammonia Over Cobalt-Based Electrocatalysts. *J. Am. Chem. Soc.* **2024**. https://doi.org/10.1021/jacs.3c13517.

(4) Liu, X.; Xu, X.; Li, F.; Xu, J.; Ma, H.; Sun, X.; Wu, D.; Zhang, C.; Ren, X.; Wei, Q. Heterostructured Bi_2S_3/MoS_2 Nanoarrays for Efficient Electrocatalytic Nitrate Reduction to Ammonia Under Ambient Conditions. *ACS Appl. Mater. Interfaces* **2022**, *14* (34), 38835–38843. https://doi.org/10.1021/acsami.2c10323.

(5) Chen, J.; Zhou, Q.; Yue, L.; Zhao, D.; Zhang, L.; Luo, Y.; Liu, Q.; Li, N.; Alshehri, A. A.; Hamdy, M. S.; Gong, F.; Sun, X. Co–NCNT Nanohybrid as a Highly Active Catalyst for the Electroreduction of Nitrate to Ammonia. *Chem. Commun.* **2022**, *58* (23), 3787–3790. https://doi.org/10.1039/D2CC00245K.

(6) Yan, J.; Liu, P.; Li, J.; Huang, H.; Song, W. Effect of Valence State on Electrochemical Nitrate Reduction to Ammonia in Molybdenum Catalysts. *Chem. Eng. J.* **2023**, *459*, 141601. https://doi.org/10.1016/j.cej.2023.141601.

(7) Tan, Z.; Du, F.; Tong, M.; Hu, J.; Zhang, N.; Huang, S.; Guo, C. Heterostructured CoS_2/MoS_2 with a Rich Active Site for an Efficient Electrochemical Nitrate Reduction Reaction to Ammonia. *Energy Fuels* **2023**, *37* (23), 18085–18092. https://doi.org/10.1021/acs.energyfuels.3c02298.

(8) Zhao, X.-E.; Li, Z.; Gao, S.; Sun, X.; Zhu, S. $CoS_2@TiO_2$ Nanoarray: A Heterostructured Electrocatalyst for High-Efficiency Nitrate Reduction to Ammonia. *Chem. Commun.* **2022**, *58* (93), 12995–12998. https://doi.org/10.1039/D2CC05204K.

(9) Xie, L.; Liu, Q.; Li, X.; Wang, G.; Ren, Z.; Qiu, H.; Sun, X.; Kong, Q. Electrochemical Reduction of Nitrate to Ammonia on an In Situ-Derived Co_3O_4@CoBi Core–Shell Nanoarray. *ACS Appl. Nano Mater.* **2024**, *7* (1), 951–956. https://doi.org/10.1021/acsanm.3c04957.

(10) Luo, Y.; Chen, K.; Wang, G.; Zhang, G.; Zhang, N.; Chu, K. Ce-Doped MoS_{2-x} Nanoflower Arrays for Electrocatalytic Nitrate Reduction to Ammonia. *Inorg. Chem. Front.* **2023**, *10* (5), 1543–1551. https://doi.org/10.1039/D2QI01798A.

(11) Niu, Z.; Fan, S.; Li, X.; Wang, P.; Liu, Z.; Wang, J.; Bai, C.; Zhang, D. Bifunctional Copper-Cobalt Spinel Electrocatalysts for Efficient Tandem-like Nitrate Reduction to Ammonia. *Chem. Eng. J.* **2022**, *450*, 138343. https://doi.org/10.1016/j.cej.2022.138343.